Nonlinear spacing and frequency effects of an oscillating cylinder in the wake of a stationary cylinder

Xiaofan Yang and Zhongquan Charlie Zheng

Citation: Physics of Fluids **22**, 043601 (2010); doi: 10.1063/1.3372169
View online: http://dx.doi.org/10.1063/1.3372169
View Table of Contents: http://scitation.aip.org/content/aip/journal/pof2/22/4?ver=pdfcov
Published by the AIP Publishing

Nonlinear spacing and frequency effects of an oscillating cylinder in the wake of a stationary cylinder

Xiaofan Yang and Zhongquan Charlie Zheng[a)]
Department of Mechanical and Nuclear Engineering, Kansas State University, Manhattan, Kansas 66506, USA

(Received 25 November 2009; accepted 16 February 2010; published online 7 April 2010)

Nonlinear responses to a transversely oscillating cylinder in the wake of a stationary upstream cylinder are studied theoretically by using an immersed-boundary method at Re=100. Response states are investigated in the three flow regimes for a tandem-cylinder system: the "vortex suppression" regime, the critical spacing regime, and the "vortex formation" regime. When the downstream cylinder is forced to oscillate at a fixed frequency and amplitude, the response state of flow around the two cylinders varies with different spacing between the two cylinders, while in the same flow regime, the response state can change with the oscillating frequency and amplitude of the downstream cylinder. Based on velocity phase portraits, each of the nonlinear response states can be categorized into one of the three states in the order of increasing chaotic levels: lock-in, transitional, or quasiperiodic. These states can also be correlated with velocity spectral behaviors. The discussions are conducted using near-wake velocity phase portraits, spectral analyses, and related vorticity fields. A general trend in the bifurcation diagrams of frequency spacing shows the smaller the spacing, frequency, or amplitude, the less chaotic the response state of the system and more likely the downstream and upstream wakes are in the same response state. The system is not locked-in in any case when the spacing between the cylinders is larger than the critical spacing. The near-wake velocity spectral behaviors correspond to the nonlinear response states, with narrow-banded peaks shown at the oscillation frequency and its harmonics in the lock-in cases. High frequency harmonic peaks, caused by interactions between the upstream wake and the downstream oscillating cylinder, are reduced in the near-wake velocity spectra of the upstream cylinder when the spacing increases. © *2010 American Institute of Physics*. [doi:10.1063/1.3372169]

I. INTRODUCTION

Wake-structure interactions among oscillating tandem cylinders can be found in many engineering applications, such as arrays of tubes in heat exchangers, power lines, and off-shore engineering structures. It is a complicated problem because the behavior of this nonlinear system depends on a combination of parameters related to both oscillating motions and tandem arrangement. This creates many nonlinear physical phenomena that are of interest to those who research fluid dynamics. The purpose of this study was to investigate how spacing and frequency influence the nonlinear behaviors of flow around the two cylinders when the downstream cylinder oscillates transversely. This study extends the current findings in the literature.[1–3] Papaioannou *et al.*[1] investigated the holes in the Arnold tongues of flow past two oscillating cylinders that oscillate simultaneously at the same amplitude and frequency. Karniadakis and Triantafyllou[2] and Zheng and Zhang[3] studied the nonlinear and frequency lock-in behaviors of a single oscillating cylinder for different frequencies and amplitudes.

Historically, a simpler version of the problem—the response of a single circular cylinder oscillating in a uniform stream—has been studied extensively using experimental measurements and numerical simulations.[4–6] Detailed mechanisms of this problem have also been reviewed.[7] Furthermore, a new development in the numerical schemes for computational studies of flow over a two-dimensional oscillating cylinder has been recently reported.[2,3,8,9] In these studies, almost every aspect in the single cylinder with/without external forcing—from vortex formation (VF) and wake structures to frequency selection and response states—has been investigated thoroughly.

The literature concerning flow over two stationary tandem cylinders includes experimental observations[7,10,11] and numerical simulations.[12–15] Physical mechanisms involved in two tandem cylinders are very different from those in a single cylinder because the wakes that are shed from both cylinders are coupled and interact with each other. The vorticity field is significantly affected by the Reynolds number ($\mathrm{Re}=UD/\nu$) and the spacing between the two cylinders. As confirmed in the literature[13] and this study, the Strouhal number ($\mathrm{St}=fD/U$) of the two tandem cylinders is not the same as that of the single cylinder for the same Reynolds number. In addition, the Strouhal number is identical for both of the cylinders in the system. Compared with single stationary cylinder cases, which are mostly dominated by Reynolds numbers, the spacing effect of the tandem cylinders is another important factor. It has been found that by changing the distance between the two cylinders wake formation and coupling may vary. Most interestingly, there exists a critical

[a)]Electronic mail: zzheng@ksu.edu.

spacing distance (S_c) on the border of the VF and vortex suppression (VS) regimes, which is marked by a sudden jump and discontinuity of the Strouhal number. For low Reynolds number laminar cases (in the range of 100 s), the critical spacing is predicted by Li *et al.*[12] to be between 3 and 4 and by Sharman *et al.*[13] to be between 3.75 and 4.

The literature concerning oscillating cylinders in the tandem arrangement is relatively scarce. Li *et al.*[16] studied numerically an oscillating cylinder in uniform flow and in the wake of an upstream stationary cylinder using a finite-element method. They mimicked the oscillation effect of the downstream cylinder by defining a sinusoidal velocity on its surface without moving the second cylinder, so that a fixed grid mesh could be used. The investigation of oscillating tandem cylinder cases was focused on only one spacing in the VF regime in that study. More recently, Papaioannou *et al.*[1] investigated the holes in the Arnold tongues of flow past two oscillating cylinders following the experimental evidence observed by Mahir and Rockwell.[17] The Arnold tongue indicates the lock-in regions in the amplitude versus frequency diagrams. It was first proven to exist in the experiment by Ongoren and Rockwell.[18] They studied the response states of a closely spaced tandem oscillating cylinders over a certain range of external forcing frequencies. The lock-in region was found to be wider than that of a single cylinder. Similar results were shown by Papaioannou *et al.*[1] using numerical simulations. At Re=160, they placed two cylinders near each other and oscillated under the same amplitude and frequency with either the same or opposite phase, and the shape of the Arnold tongue was clearly shown in their study. Several types of nonlinearity appeared in the velocity phase portrait, from lock-in, quasiperiodic, and transitional to period doubling. They also studied two spacing distances (2.5 and 3.5) that could be related to the critical and VF regimes correspondingly, with a restriction of both of the cylinders oscillating at the same amplitude and frequency. The spacing and frequency effects on nonlinear behavior of a tandem cylinder system with two cylinders are therefore the focus of the current study that includes all of the three regimes of VS, critical, and VF regimes. It should also be noted that because the two cylinders in the current study are not in the same oscillating motion, many aspects of flow are different from those in Papaioannou *et al.*[1] A primary difference is that the flow field behind the first cylinder can be very different from that behind the second cylinder in both frequency response and phase portrait. We found new vortex structures in the wake related to different nonlinear response states.

While the response of a tandem cylinder system to a controlled oscillating downstream cylinder with a prescribed frequency is studied in the paper, there are many practical applications on flow around self-oscillating cylinders due to vortex-induced vibration.[19–21] However, under certain conditions, some of the flow behaviors in controlled vibration can be very close to those in free vibration.[22,23]

The numerical scheme of the immersed-boundary method (IBM) is explained in Sec. II. In Sec. III, the flow patterns of a system of two stationary cylinders at different spacing and the related Strouhal number effect are described.

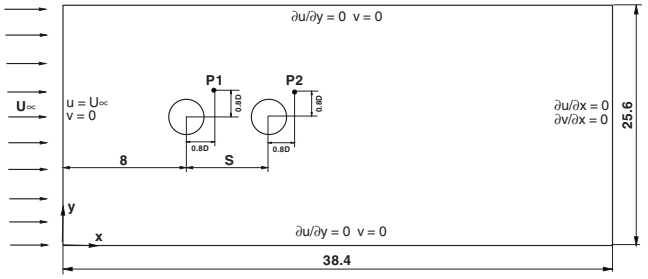

FIG. 1. Computational domain, boundary conditions, and near-wake velocity probing points.

A detailed discussion on the oscillating downstream cylinder cases is presented in Sec. IV, and the conclusions are made in Sec. V.

II. NUMERICAL SIMULATION

Direct numerical simulations based on an improved IBM with direct forcing[24] are carried out to simulate the flow system. The nondimensionalized governing equations using the characteristic parameters of ρ, U, and D for two-dimensional, laminar, incompressible flow are

$$\nabla \cdot \mathbf{u} = 0 \tag{1}$$

and

$$\frac{\partial \mathbf{u}}{\partial t} + \mathbf{u} \cdot \nabla \mathbf{u} = -\nabla P + \frac{1}{\mathrm{Re}} \nabla^2 \mathbf{u} + \mathbf{f}, \tag{2}$$

where Re is defined as UD/ν, with U the uniform incoming velocity, D the cylinder diameter, and ν the kinematic viscosity. A Re of 100 is used for this study. The boundary forcing term $\mathbf{f}$ is applied on an internal layer of the immersed boundary and calculated at each time step to obtain the desired boundary velocity by using the formula

$$\mathbf{f} = \mathbf{S} + \nabla P - \frac{1}{\mathrm{Re}} \nabla^2 \mathbf{u} + \frac{1}{\Delta t} (\mathbf{v} - \mathbf{u}), \tag{3}$$

where $\mathbf{v}$ is the desired velocity and $\mathbf{S}$ is the convection term defined as $\mathbf{S}=(\mathbf{u}\cdot\nabla)\mathbf{u}$. The internal layer is a layer of grid points that are immediately interior to each of the cylinder surface boundaries.

The momentum equation, Eq. (2), is solved using a second-order differencing scheme on a staggered Cartesian grid, which includes a semi-implicit scheme for the diffusion term (with the normal direction diffusion terms being the Crank–Nicholson scheme), the Adams–Bashforth scheme for the convection, and second-order central differencing for diffusion. The incompressibility condition, Eq. (1), is satisfied by solving a Poisson equation for pressure correction using FISHPACK. The overall accuracy of the scheme is able to reach the second order. More details concerning the modified IBM can be found in Zhang and Zheng.[24]

When the IBM is used, arbitrary shapes and motions of solid bodies can be effectively simulated by a proper construction of the boundary forcing term so that a simple, nonmoving Cartesian grid can be used. The domain size selected for this study is 38.4×25.6, as shown in Fig. 1. The up-

stream cylinder is located at 8, sufficiently away from the inlet boundary to eliminate the inlet effect. The distance between the two cylinders is defined as S (nondimensionalized by the cylinder diameter D). The outlet boundary is also far enough from the downstream cylinder to allow the vortex street to develop fully. The grid-size independence check[24] determined that a grid size with $\Delta x=\Delta y=0.025$ provides an acceptable grid resolution for all the computational cases at Re=100. The boundary conditions are also shown in Fig. 1. For a stationary cylinder, the velocity on the surface is zero. For a transversely oscillating cylinder, the displacement is calculated as

$$d_y = A\ \sin(2\pi t * f_c), \tag{4}$$

where A (nondimensionalized by D) is the amplitude of the displacement, f_c is the forcing frequency, and t is the time. The time step size is computed from different forcing frequencies as $\delta t=1/f_cN$, where N is the number of time steps within one oscillation period. Moreover, the size of the time step must also satisfy the stability criterion of an explicit scheme for a two-dimensional convection-diffusion equation, that is, $\delta t<\min[h^2\ \mathrm{Re}/4, 2/(u^2+v^2)\mathrm{Re}]$, where h is the grid size.

The computational scheme has been verified with numerous experimental and computational data.[24] For example, for flow over a single oscillating cylinder, the computational results at various forcing frequencies were shown in Zheng and Zhang,[3] where both frequency lock-in and non-lock-in cases were identified using time histories and power spectra of lift and drag, and good agreements were achieved in comparison to literature data.[5,6,9,18] These examples have provided sufficient validations for the computational scheme used in our study.

In order to justify the two-dimensional flow assumption in this study, we have tested three-dimensional simulation at Re=100 with a periodic boundary condition in the cylinder axial direction. By examining the vorticity contours and velocity field in several cutting planes perpendicular to the cylinder axial direction, we have found that the flow remains two dimensional, with the variation range of these variables less than 1% along the axial direction. We also increased Reynolds number to 160, which is a case that was treated as two-dimensional tandem cylinders,[1,15] and the three dimensionality started to show. Oscillation of the downstream cylinder does not enhance the three-dimensional effect much. Therefore, it is expected that the Reynolds number for flow to become three dimensional could be lower in a tandem cylinder system than that in a single cylinder system [where Re=188.5 (Ref. 25)], with a possibility that oscillation could further reduce that Reynolds number. Considering the stabilizing and destabilizing effects of the downstream cylinder,[15] this Reynolds number may also vary with the separation distance between the two cylinders. Although for the purpose of this study we do not intend to determine this Reynolds number, based on our simulation this Reynolds number can possibly be below 160. Also, the case we study here at Re=100 is still within a safe range for flow to be two dimensional, hence formation due to instability in the axial direction is not considered.[26]

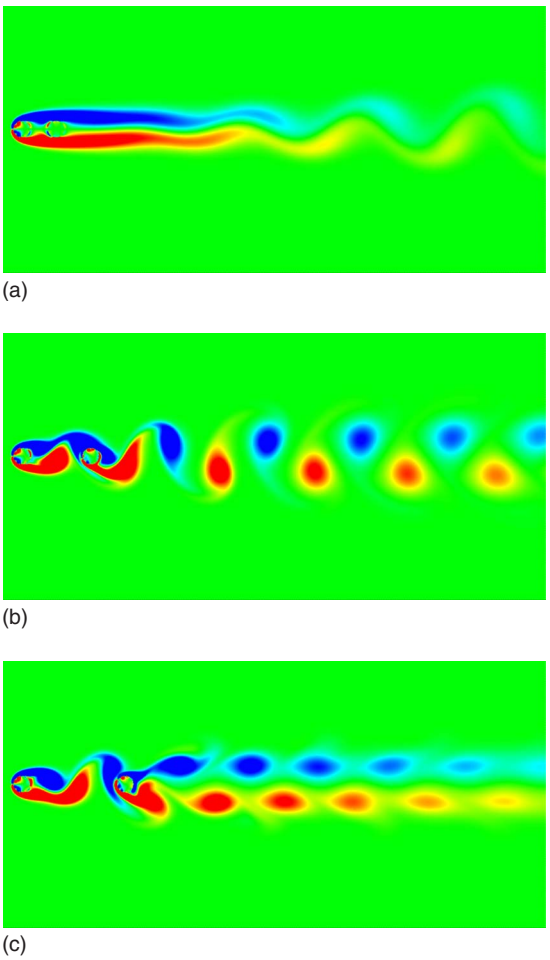

FIG. 2. (Color online) Vorticity field for a stationary tandem cylinder system at three different spacing distances: (a) $S=2$ (VS), (b) $S=4$ (critical), and (c) $S=6$ (VF).

III. FLOW PATTERNS FOR FLOW OVER TWO STATIONARY TANDEM CYLINDERS

Complicated flow patterns in a stationary tandem cylinder system have been demonstrated in the literature.[7,10,11,13] Basically, the flow patterns can be divided into two regimes by a "critical spacing" (S_c). In the case of Re=100, the value of S_c is between 3.75 and 4, according to Sharman *et al.*[13] The different types of vortex streets are shown in the vorticity contours for Re=100 in Fig. 2. When $S<S_c$ ($S=2$ in Fig. 2), the flow is in a regime called the "VS regime," in which the wakes behind both cylinders are rather weak, and there is almost no vortex shedding, neither in between nor behind the cylinders other than a low-frequency wavy flow pattern in the wake. The downstream cylinder is so close to the upstream one that formation of vortices is hindered. The shear layer from the upstream cylinder does not have sufficient room to form shed vortices, although there is no precise relation between the VF length in the wake of a single cylinder and the critical spacing of a tandem cylinder system.[15] The stabilized wake behind the upstream cylinder (in the sense of a Hopf bifurcation[25]), due to the closeness of the downstream cylinder, further stabilizes the wake from the second cylinder so that there is no clear vortex shedding even in the wake

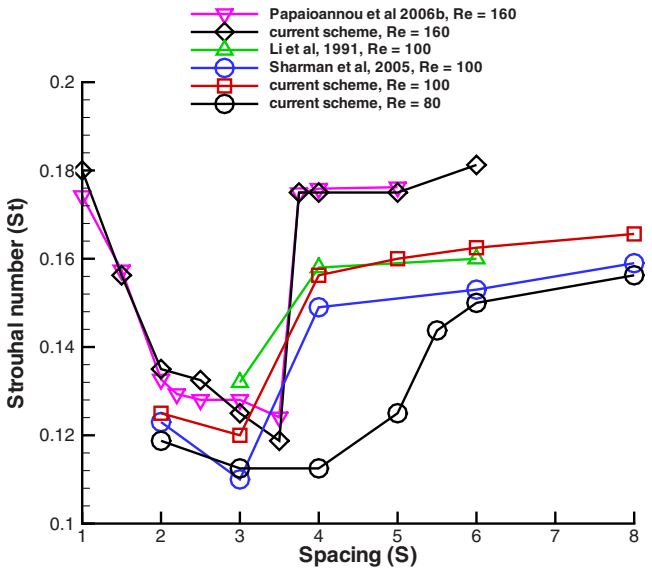

FIG. 3. (Color online) Comparisons of Strouhal number prediction for a stationary tandem cylinder system at different spacing distances (S) and Reynolds numbers of 80, 100, and 160.

after the downstream cylinder. When approaching the critical spacing, the vortex shedding upstream to the second cylinder is intermittent. After a transient period, at $S=S_c$ ($S=4$ in Fig. 2), a synchronized vortex street is formed eventually behind the downstream cylinder, and a sudden jump in the Strouhal number ($\mathrm{St}=fD/U$) for the cylinder system occurs, although there is still no clear vortex shedding between the cylinders. It should be noted that this Strouhal number is for the entire tandem cylinder system and includes interference effects among the two cylinders and their wakes, which is not the same as that for a single cylinder. This sudden jump is indicative that the spacing is reaching the critical spacing. When $S>S_c$ ($S=6$ in Fig. 2), the flow is in the "VF regime," in which synchronized vortex shedding occurs and well developed vortices are shed from the upstream cylinder and reattach themselves to the downstream one. The shedding vortices behind the first cylinder join those from the downstream cylinder to form a coupled vortex street in the wake of the tandem cylinder system.

Figure 3 shows the computed Strouhal number versus the spacing distance at Re=100 and two other Reynolds numbers at 80 and 160 for comparison. The reason to end at Re=160 is because of three dimensionality at high Reynolds number flow stated in Sec. II. On the other hand, at further lower Reynolds numbers, such as Re=50 as we tested, the flow is at the verge of being a steady state with a long wake formation length for a single cylinder case. The possible stabilizing effect of the downstream cylinder can make the flow even more stable, and therefore the VF regime is large and no vortex shedding is shown in this regime. In our computation, the Strouhal number is calculated after the periodic vortex streets are formed and the solution converges to a state that shows periodic oscillations. The average surface pressure coefficient history, during the periods after a converged solution (80 or 160 depending on the frequency resolution needed) is established, is then used for spectral analysis to determine the Strouhal number. Our St values at Re=100 fit between those reported by Sharman *et al.*[13] and Li *et al.*[12] The sudden jump of the Strouhal number occurs at $S=4$ in all of the three data sets. For another Reynolds number of 80, we also repeated the same procedure and obtained the critical spacing around 5.5, as shown in Fig. 3, which agrees well with the result by Tanida *et al.*,[11] but is different from the value of 3.7 reported by Li *et al.*[16] One of the reasons could be the resolutions of the grid mesh. As for the single cylinder case with Re=100, a relatively coarse mesh was used by Li *et al.*[16] that gave the value of St as 0.166, a bit lower than the usual value of 0.17 reported in the literature. Another reason could be due to different definitions of the critical spacing. There are several different ways of determining the critical spacing in the literature. We define the critical spacing by observing the sudden increase in the Strouhal number, which is the same definition as what used by Sharman *et al.*[13] In Li *et al.*[16] the wake length change as an indicator of separate flow regimes was used, while in Tanida *et al.*[11] the interference drag was used as the criterion.

IV. SPACING AND FREQUENCY EFFECTS OF A TRANSVERSELY OSCILLATING DOWNSTREAM CYLINDER

Oscillations of the downstream cylinder create more complicated nonlinear behaviors and add two more parameters to the stationary tandem cylinder system: the frequency and the amplitude of the oscillating downstream cylinder. In this study, we investigated different oscillating frequencies at various spacings under relatively small amplitudes. It should be noted that oscillations of cylinder do not alter the spacing range significantly in distinguishing the VS and VF regimes, as long as the oscillation amplitude is small such as those in this study. In terms of phase portrait of velocity field, in a stationary tandem cylinder system there is always a "lock-in" type in the phase portrait of both downstream and upstream wakes, since there is only one major characteristic frequency in the system corresponding to the Strouhal number of the stationary tandem system.

In the following discussions, we analyze nonlinear behaviors for each case (at a specific spacing, frequency, and amplitude) in three ways: (1) phase portrait plots to analyze the nonlinear dynamic mechanism; (2) power spectral analyses to reveal frequency effects; and (3) vorticity contour plots to explain the flow physics and vortex patterns.

Velocity histories are recorded at two points that are both $0.8D$ downstream of the center of each cylinder and $0.8D$ above the center line in the transverse direction (P1 and P2 shown in Fig. 1). These points are in the near-wake region and thus the effects from vortex shedding and oscillations of the cylinder can be easily detected. For P1, we can detect the behaviors in the wake of the upstream cylinder, while for P2, the merging effect of the vortex streets of the two cylinders can be seen. Power spectral analyses are carried out using the histories of streamwise velocity in the last several periods. The dominant frequencies in the spectra can be used as one of the indicators for classifying the nonlinear response states. In the phase portrait plots, the trajectories of time histories of

the streamwise (u) and the transverse (v) velocity components are mapped into the u-v plane to identify the limit cycles for characterizing responses of the nonlinear system under forcing. For the problems of flow over cylinders, phase portraits of velocity have been used to categorize nonlinear response states.[1,2,16]

In this study, the spacing between the two cylinders is considered a major factor that influences system behaviors, which differs from a previous study[1] where frequency and amplitude were the main factors. At one oscillating frequency, under different spacing distances, the resulting flow patterns change. On the other hand, how the flow patterns vary with the oscillating frequencies is also highly influenced by the spacing distance between the two cylinders. Here we study three spacing distances of $S=2$, 4, and 6, which correspond to the VS, critical, and VF flow regimes in the stationary tandem cylinder case, as discussed in Sec. III. For each of the spacing S, six different oscillating frequencies were tested: natural vortex shedding frequency (f_{ns}), two nearby frequencies ($f_c=0.9f_{ns}, 1.1f_{ns}$), and three higher-frequency excitations ($f_c=1.3f_{ns}, 1.5f_{ns}, 1.7f_{ns}$). The oscillating displacement amplitude A was fixed at two relatively small values of 0.15 and 0.35.

It should be noted that the natural frequency here, f_{ns}, is the same as the Strouhal number of the corresponding stationary tandem cylinder system, a term also used in the literature.[1] In this study, the intention is to investigate the response of the system to oscillations in the vicinity of this frequency. Therefore, the oscillation frequency f_c is scaled by the natural frequency.[1] This natural frequency changes with the spacing between the two cylinders, as shown in Fig. 3, because the system characteristics change.

In this discussion, we first give an overall picture of the nonlinear behaviors of the system by showing bifurcation diagrams of normalized frequency (with respect to the corresponding natural frequency) versus spacing in Figs. 4 and 5, drawn from the cases of different combinations of above mentioned parameters. The diagrams categorize all the cases into three states or classes: lock-in, transitional, and quasiperiodic, the same three classes used by Papaioannou *et al.*[1] However, unlike the study by Papaioannou *et al.*[1] in which the cylinders have the same motion (although either perfectly in phase or in opposite phase), we have one forced oscillating cylinder and one stationary cylinder. We also distinguish, with filled or hollow symbols, whether there are peaks at high frequencies in the velocity spectra detected in the wake behind the upstream cylinder, a feature that is shown in the streamwise velocity spectra in Figs. 6 and 7 and will be further discussed in Secs. IV A–IV C. In addition, we inspect both the velocities behind the upstream cylinder (at P1) and the downstream cylinder (at P2) because flow in the downstream wake may not necessarily behave the same way as it does in the upstream wake. According to the results to be discussed later, the flow patterns in the two wakes can belong to different categories among the three states. Even when flows at P1 and P2 are in the same state, differences in spectra still exist. It is physically plausible that the upstream and downstream flows can be in the same class because of the incompressible, elliptic-type domain of influence, particularly when the spacing distance between the two cylinders is small. However, differences in flow features also exist due to different wakes behind the upstream cylinder with respect to each of the flow regimes. Particularly, if the distance between the two cylinders is sufficiently large, the differences are more likely to occur.

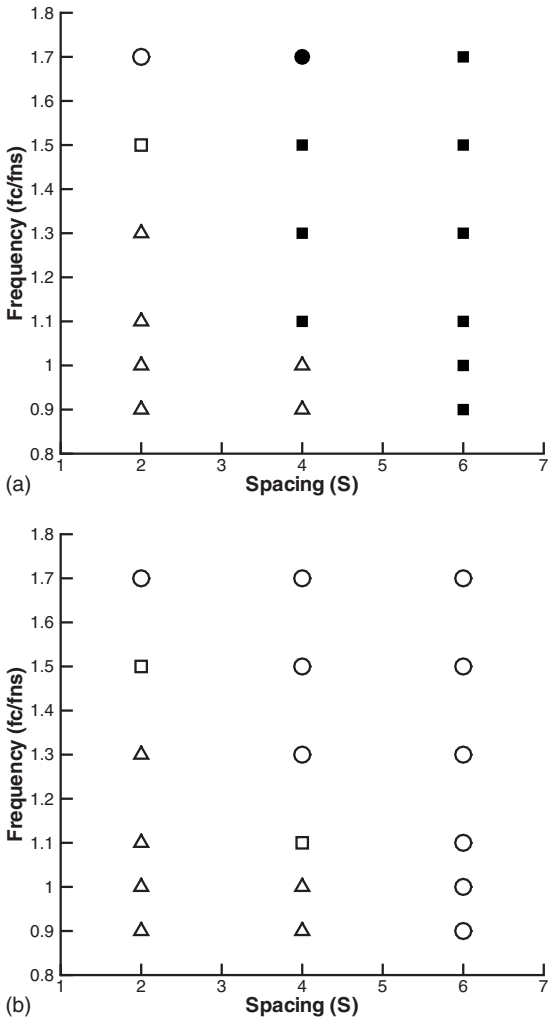

FIG. 4. Response state diagrams of spacing vs frequency for probed velocities in the wake of each of the cylinders at $A=0.15$. (a) Upstream cylinder; (b) downstream cylinder. Triangle: lock-in; square: transitional; circle: quasiperiodic. The filled symbols indicate that wake velocity spectra of the upstream cylinder lose peaks at high frequencies.

The general trend illustrated in the diagrams shows that the smaller the spacing, frequency, and amplitude, the more likely the system is locked-in, and thus the bifurcation diagrams of frequency spacing do not form Arnold tongues. By comparing Fig. 4(a) with Fig. 4(b) and Fig. 5(a) with Fig. 5(b), we see that it is more likely that the upstream wake and downstream wake are in the same flow pattern class when the spacing is smaller and excitation frequency is lower. In addition, no high-frequency peaks appear in the upstream wake in the non-lock-in cases at the critical spacing and in all cases at the VF spacing. As long as the flow state is a lock-in, the upstream high-frequency peaks remain. The high-frequency peaks in the downstream wake are generated by interactions between the upstream wake and the oscillat-

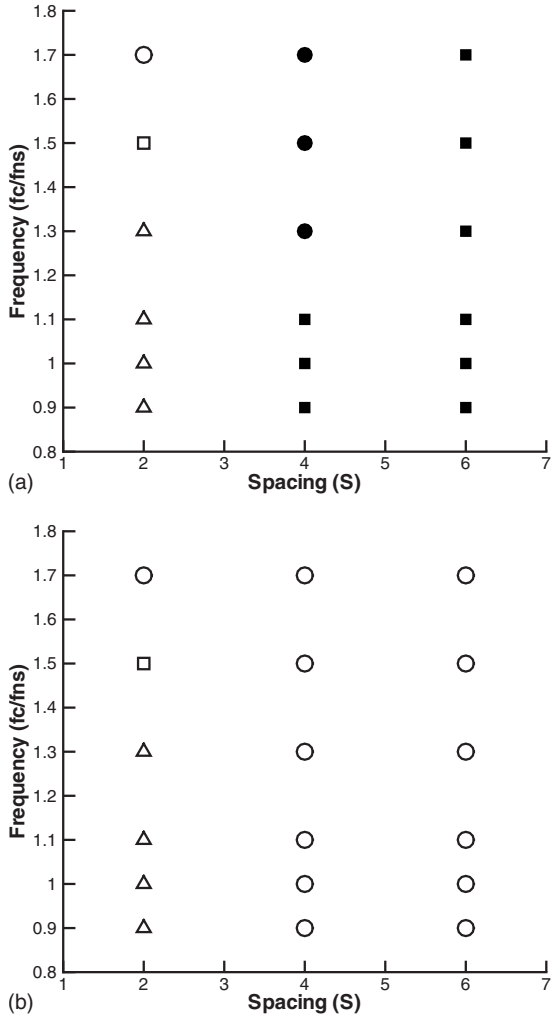

FIG. 5. Same as in Fig. 4 but with $A=0.35$.

ing downstream cylinder. This explains why the high-frequency peaks no longer exist in the upstream wake at some critical and all VF spacing, because such interactions only weakly affect the upstream wake when the spacing is large. At the VS spacing, as the two cylinders are very close, the oscillatory flow effect due to the oscillating downstream cylinder is very strong, leading to high-frequency peaks in all the VS ($S=2$) cases. At the VF spacing, high-frequency peaks disappear in the upstream wake in all of the cases, while at the critical spacing, only the two lock-in cases at the lower amplitude in Fig. 4 do not show this phenomenon. Changing amplitudes does not affect either the VS cases or the VF cases, but does affect significantly the critical spacing cases, resulting in no lock-in for all the critical spacing cases at the larger amplitude. Therefore, critical spacing ($S=4$) is sensitive to excitation amplitude, which leads lock-in and transitional cases at the lower amplitude to either transitional or quasiperiodic at the higher amplitude. In a large spacing system of VF ($S=6$) cases, the upstream wake remains transitional and the downstream wake remains quasiperiodic, regardless of the frequency or the amplitude of the excitation. We also studied the state bifurcation diagrams for a lower Reynolds number case at $Re=80$ (in which case the critical spacing is at $S=5.5$, as discussed in Sec. III), and they are all in the same general trend as in the above descriptions for $Re=100$.

Upon further inspection of the detailed frequency response behaviors at each spacing distance, we find that the spectral contents of near-field velocity histories, Figs. 6 and 7, can also be linked to the three states as (1) for lock-in, there is a clear, narrow-banded dominant peak at f_c and its harmonics; (2) for transitional, there is a major, relatively broadband peak close to f_c or f_{ns}, and other peaks are in a scattered and insignificant manner; and (3) for quasiperiodic, there are peaks at both f_c and f_{ns}, and also peaks at their respective harmonics.

In Secs. IV A–IV C, we look into the frequency response behaviors presented in power spectrum plots at each spacing distance along with the phase portrait plots to confirm the compatibility among them in terms of classifying the response states. Furthermore, corresponding vortex shedding patterns in vorticity contour plots are also discussed in the context of response states.

A. The VS spacing, $S=2$

At the VS spacing ($S=2$), the two cylinders are in a very close arrangement. Unless the amplitude is sufficiently high, the existence of the downstream cylinder hinders the development of vortex shedding in the wake of the upstream cylinder. The wake of the upstream cylinder is "forced" to oscillate with that of the downstream cylinder, resulting in the same response between the two wakes. Furthermore, as flow oscillations in the VS cases are closely coupled between the upstream and downstream regions, the flow is locked-in in a wide frequency range, and flow patterns behind the two cylinders fall into the same flow class. The entire tandem cylinder system is thus similar to a single bluff body under oscillatory excitations. In the frequency-spacing diagrams in Figs. 4 and 5, at $0.9f_{ns}$ to $1.3f_{ns}$, pure lock-in responses exist, which break down to quasiperiodic states at higher frequencies. The two different amplitudes result in the same type of responses, and increasing the amplitude further may break down lock-in at a lower frequency.

When flow is locked in, significant peaks appear at the excitation frequency and its superharmonics. For example, in the case of $f_c=1.3f_{ns}$, one dominant peak appears at $1.3f_{ns}$ in the wake behind each cylinder, as shown in Figs. 6 and 7. There are no peaks at either f_{ns} or its superharmonics. A limit cycle of a single closed orbit in Figs. 8(a) and 8(b) is repeated in time in the velocity phase portrait plots for both upstream and downstream wakes, indicating a pure lock-in for flow around both cylinders. Note that the numbers on both the abscissa and ordinate of all the phase portraits in this paper are in the unit of dimensionless velocity. Since this system behaves similarly to a single oscillating bluff body, vorticity contours in Fig. 8(c) show a typical 2S vortex shedding structure (Ref. 5), in which each positive vortex is followed by a negative vortex behind the downstream cylinder. This vortex shedding pattern was also observed[3] for single oscillating cylinder cases in the lock-in regime.

For frequencies higher than $1.3f_{ns}$, the excitation frequency f_c is away from the natural frequency f_{ns}. The re-

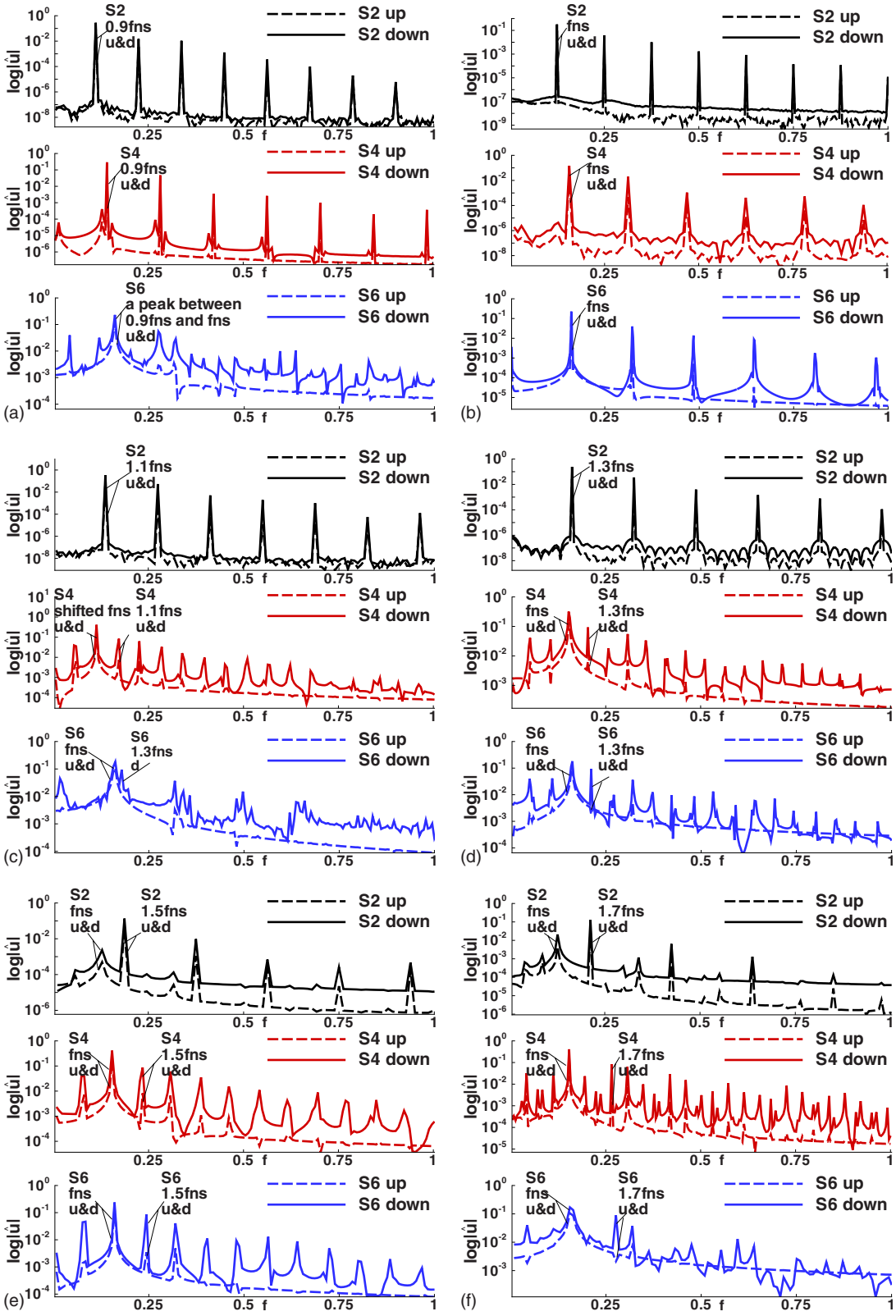

FIG. 6. (Color online) Velocity power spectra at the two locations P1 (upstream, dash line) and P2 (downstream, solid line) with primary peaks pointed out either at the upstream spectrum (u) or downstream spectrum (d) or both (u and d). Excitation amplitude $A=0.15$ with different excitation frequencies at (a) $f_c=0.9f_{ns}$, (b) $f_c=f_{ns}$, (c) $f_c=1.1f_{ns}$, (d) $f_c=1.3f_{ns}$, (e) $f_c=1.5f_{ns}$, and (f) $f_c=1.7f_{ns}$.

sponse state first changes to a transitional state when dominant peaks start to appear at frequencies either f_c or f_{ns}, or between the two, and then the state turns to quasiperiodic in which significant peaks appear at both f_c and f_{ns} and their superharmonics. However, as the entire flow field is closely synchronized, the near wakes behind the upstream and downstream cylinders are again in the same flow class. We look at the case of $f_c=1.7f_{ns}$, $A=0.15$ as an example of the

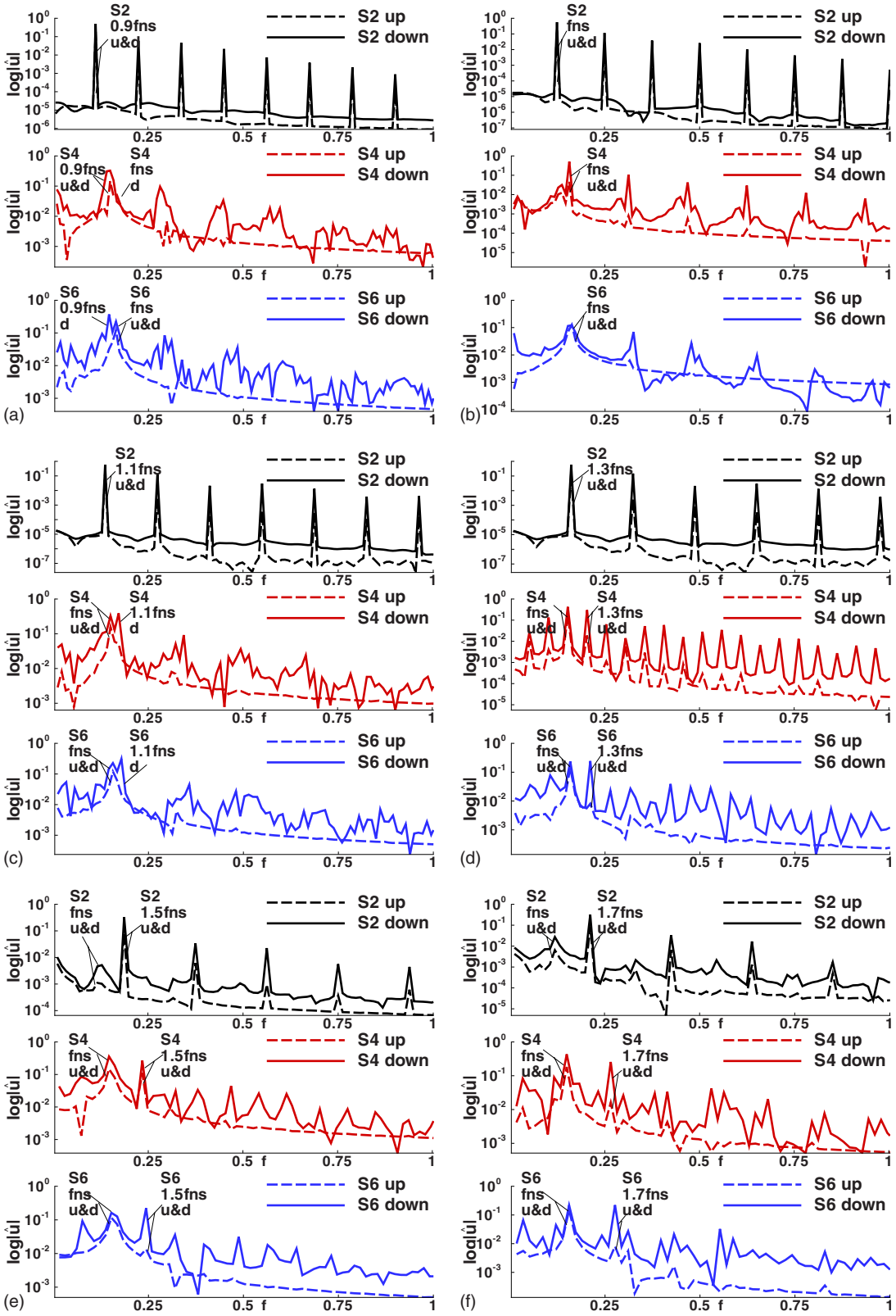

FIG. 7. (Color online) Same as in Fig. 6, but excitation amplitude $A=0.35$, with the same excitation frequencies at (a) $f_c=0.9f_{ns}$, (b) $f_c=f_{ns}$, (c) $f_c=1.1f_{ns}$, (d) $f_c=1.3f_{ns}$, (e) $f_c=1.5f_{ns}$, and (f) $f_c=1.7f_{ns}$.

quasiperiodic situation. In Fig. 6, the spectra show that both upstream and downstream wakes have peaks at identical frequencies of f_c and f_{ns} and their superharmonics, which means that the flow in both regions is quasiperiodic. In Figs. 9(a) and 9(b), the velocity phase portrait plots also display a quasiperiodic pattern. However, in the vorticity contours in Fig. 9(c), the downstream far wake still develops into a 2S vortex structure. In the near wake the 2S structure is different, where positive and negative vortices are not shed one by one but form two parallel rows. This behavior still belongs to

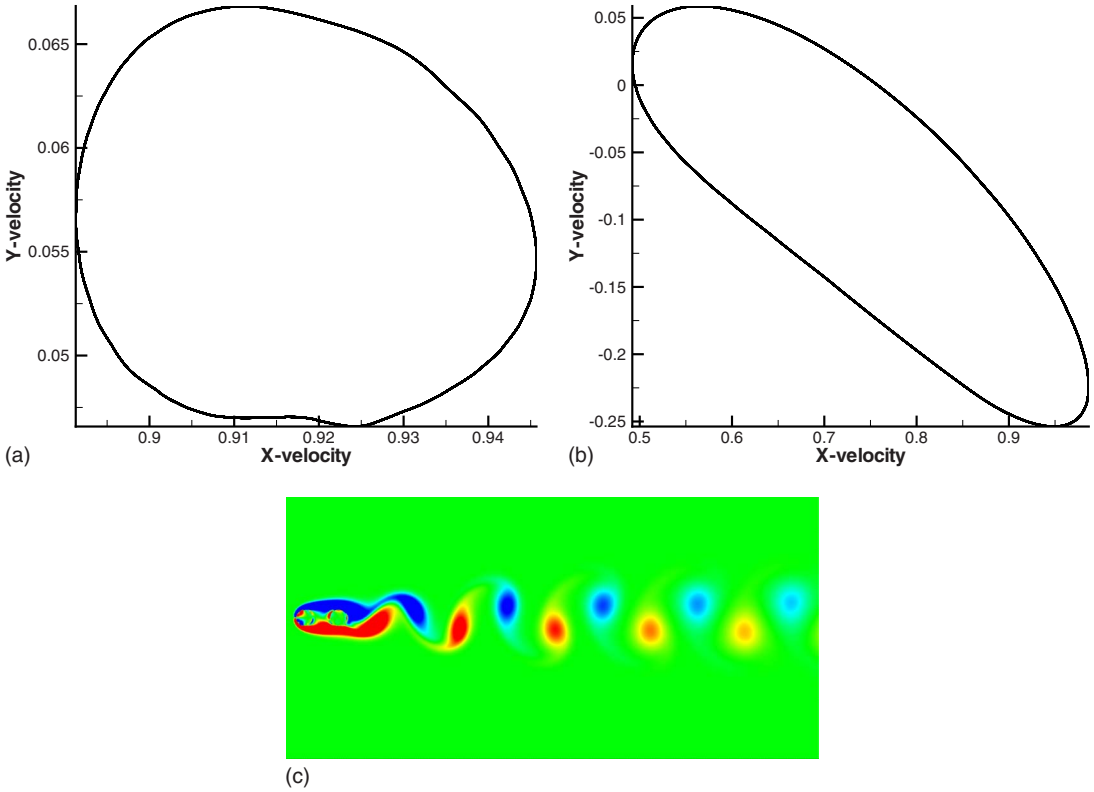

FIG. 8. (Color online) The VS case of $S=2$, $f_c=1.3f_{ns}$, and $A=0.15$. (a) Phase portrait plot (upstream cylinder), (b) phase portrait plot (downstream cylinder), (c) vorticity contour plot.

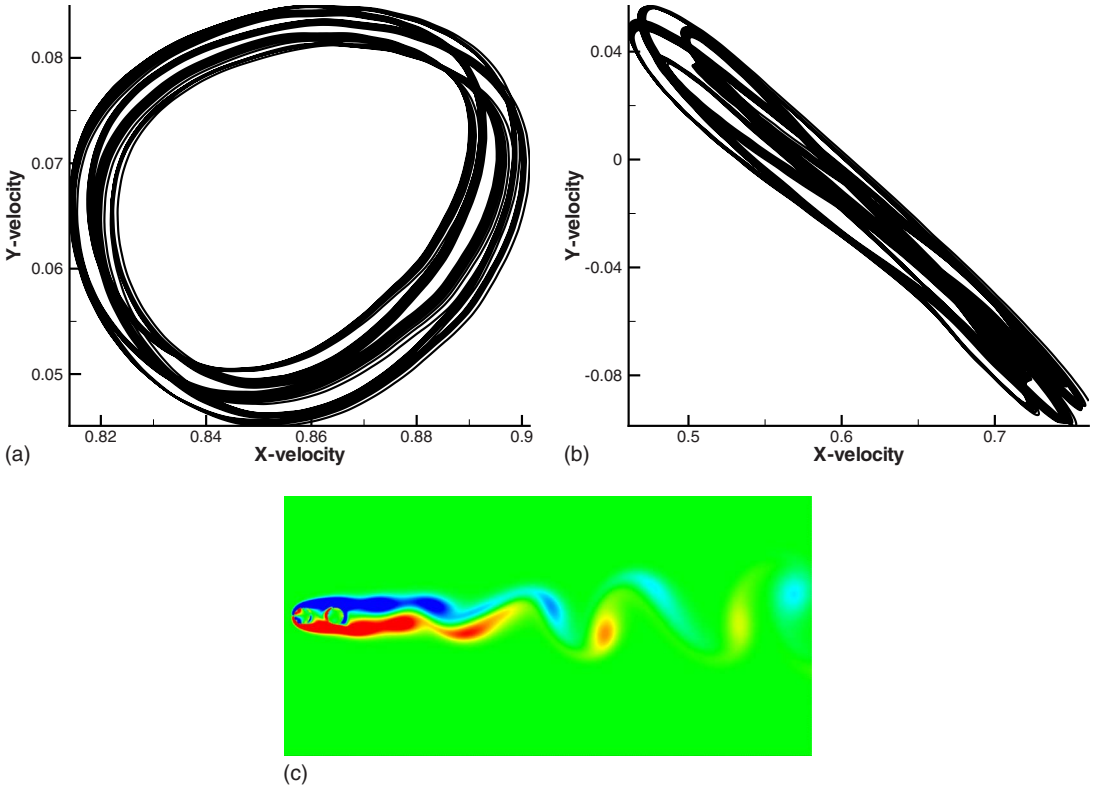

FIG. 9. (Color online) The VS case of $S=2$, $f_c=1.7f_{ns}$, and $A=0.15$. (a) Phase portrait plot (upstream cylinder), (b) phase portrait plot (downstream cylinder), (c) vorticity contour plot.

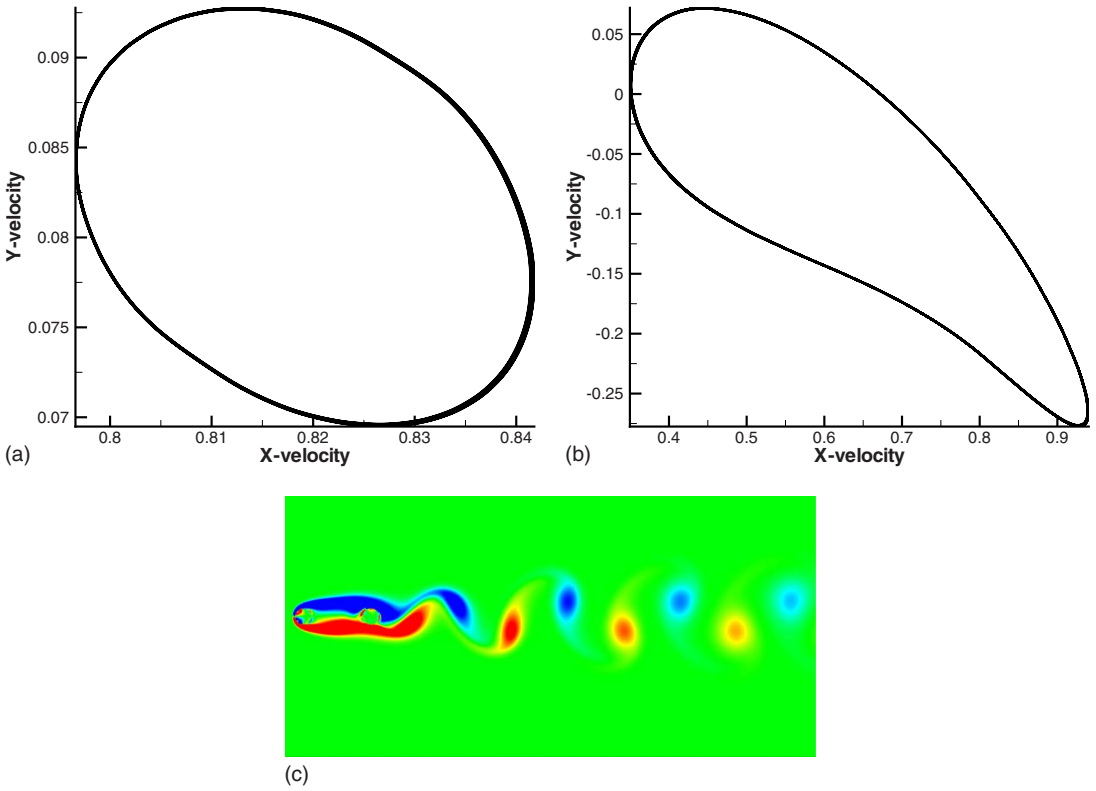

FIG. 10. (Color online) The critical spacing case of $S=4$, $f_c=0.9f_{ns}$, and $A=0.15$. (a) Phase portrait plot (upstream cylinder), (b) phase portrait plot (downstream cylinder), (c) vorticity contour plot.

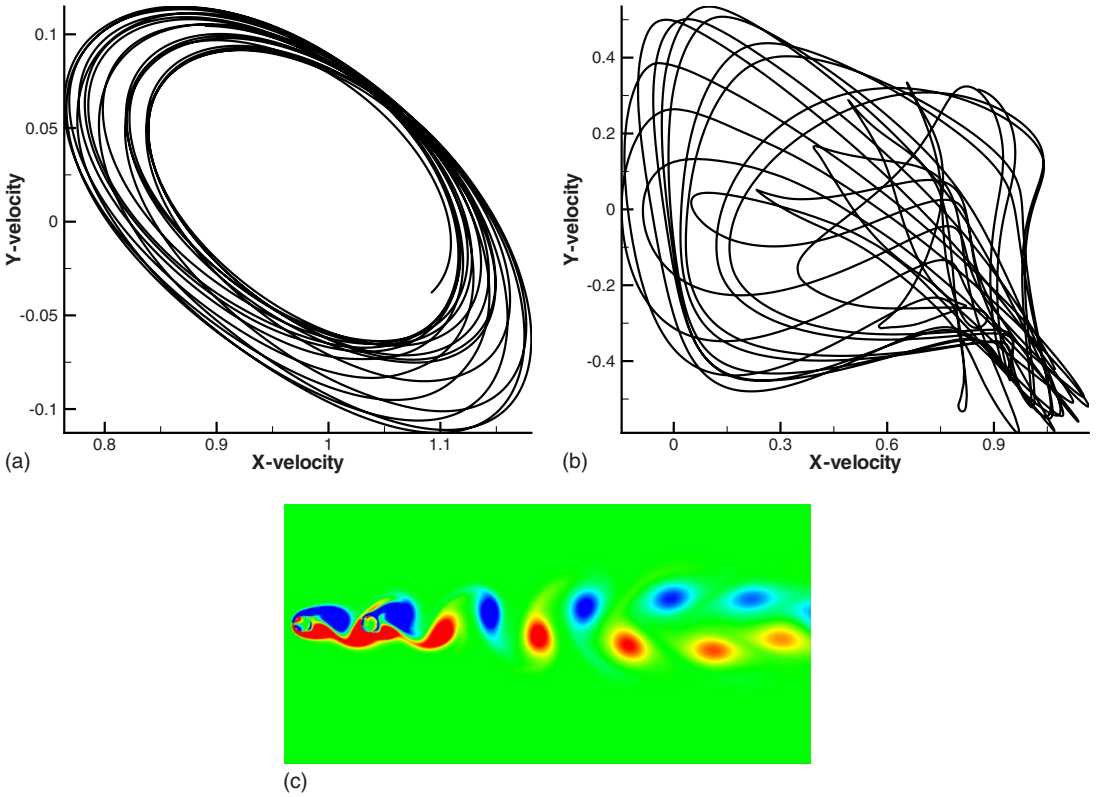

FIG. 11. (Color online) The critical spacing case of $S=4$, $f_c=0.9f_{ns}$, $A=0.35$. (a) Phase portrait plot (upstream cylinder), (b) phase portrait plot (downstream cylinder), (c) vorticity contour plot.

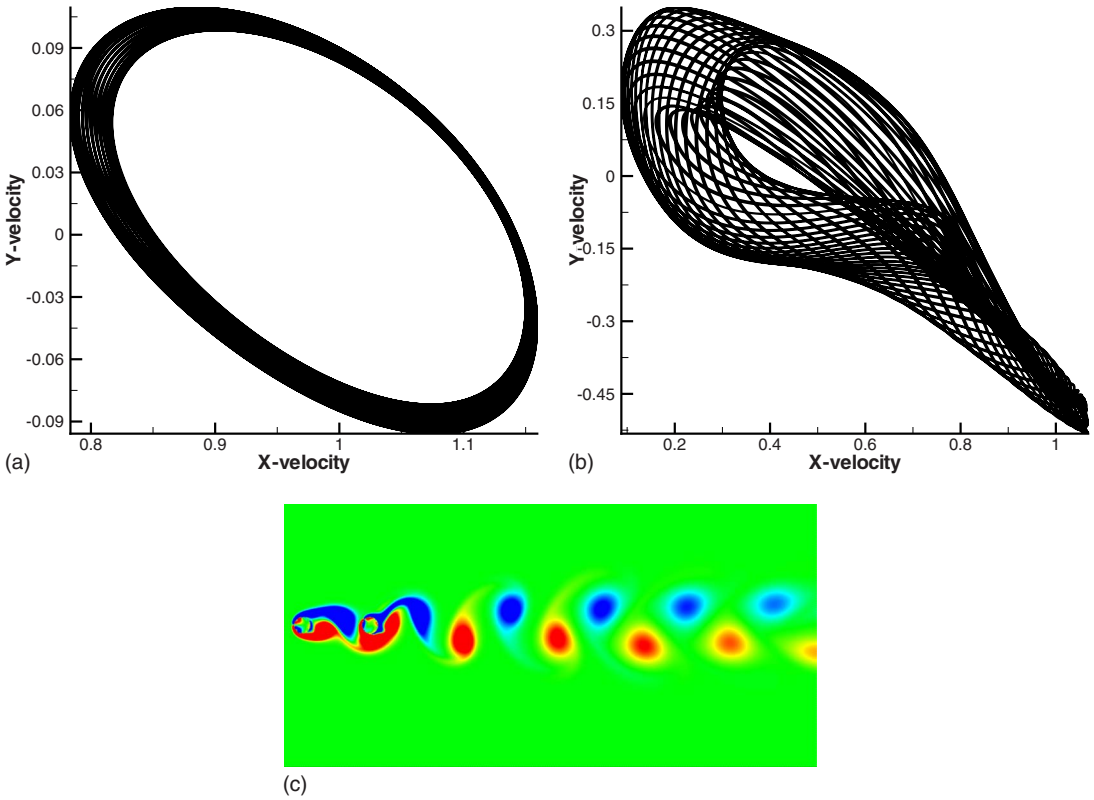

FIG. 12. (Color online) The critical spacing case of $S=4$, $f_c=1.3f_{ns}$, and $A=0.15$. (a) Phase portrait plot (upstream cylinder), (b) phase portrait plot (downstream cylinder), (c) vorticity contour plot.

the 2S structure. However, in order to distinguish it from a typical 2S vortex street, we name it 2S*. The somewhat organized vortex structures are not typical for a quasiperiodic case in which a more chaotic flow field is usually expected.

Similarity between a VS tandem cylinder system with a downstream oscillating cylinder and a single oscillating cylinder is also evident in the velocity phase portrait plots. We used cases reported by Zheng and Zhang[3] as examples to compare. In their study, a uniform flow passes a single cylinder that oscillates with the same displacement function as Eq. (4) at a Reynolds number of 200, while other parameters remain the same as in this study. We compared near-wake velocity phase portraits of lock-in and non-lock-in single cylinder oscillations with those corresponding lock-in and non-lock-in VS cases here. We found that for the lock-in single cylinder oscillation cases, the phase portraits had a similar orbital trace as the VS lock-in cases, such as those shown in Fig. 8, while the single cylinder non-lock-in cases had similar chaotic and disordered phase portrait plots as the non-lock-in VS case in Fig. 9.

With respect to effect of different oscillating amplitudes on flow behavior, our study shows that increasing the oscillating amplitude from 0.15 to 0.35 does not change the frequency responses and other flow features at the VS spacing. This is compatible with Fig. 1(c) in Ref. 1, which also shows that the system stays locked-in under a broad range of oscillating amplitudes.

B. The critical spacing, $S=4$

Unlike the VS cases, at this spacing, the system becomes more sensitive and easier to change from lock-in to other states. Because of this spacing, the vortex wake from the upstream cylinder is at the beginning of being fully developed. In the frequency versus spacing diagrams in Figs. 4 and 5, under $A=0.15$, three kinds of frequency responses all appear, and when the amplitude is increased to 0.35, no lock-in cases occur whatsoever. In the two lock-in cases, the response states of the upstream and downstream cylinders are still the same, as in the VS lock-in cases. However, when the system is not locked-in, different responses occur in the near wakes of the two cylinders, which is not the case as in the close spacing VS cases.

In a lock-in case with the critical spacing, such as $A=0.15$ and $0.9f_{ns}$, the frequency response of velocity spectra behaves the same as those of all the VS lock-in cases, as evident in Figs. 6 and 7. That is, as shown in Fig. 6(a) for $S=4$, only major peaks appear at the excitation frequency and their harmonics in the velocity spectra of both cylinders. Because of the same spectral behavior, the phase portraits and vorticity contours of a lock-in case with the critical spacing in Fig. 10 are also very similar to those of the VS lock-on cases, such as those shown in Fig. 8: the phase portraits of velocity at P1 and P2 are clearly single close orbits, and the downstream vortex street has the 2S pattern. In this case of the critical spacing with $A=0.15$ and $0.9f_{ns}$, the upstream

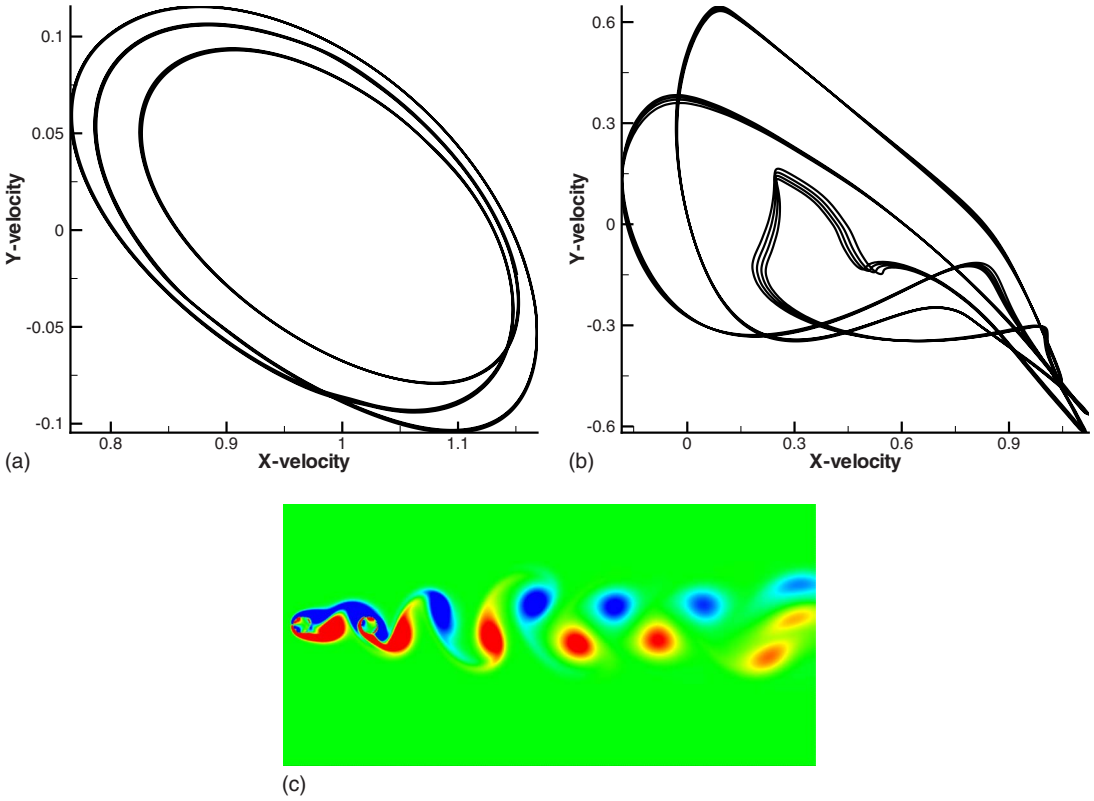

FIG. 13. (Color online) The critical spacing case of $S=4$, $f_c=1.3f_{ns}$, and $A=0.35$. (a) Phase portrait plot (upstream cylinder), (b) phase portrait plot (downstream cylinder), (c) vorticity contour plot.

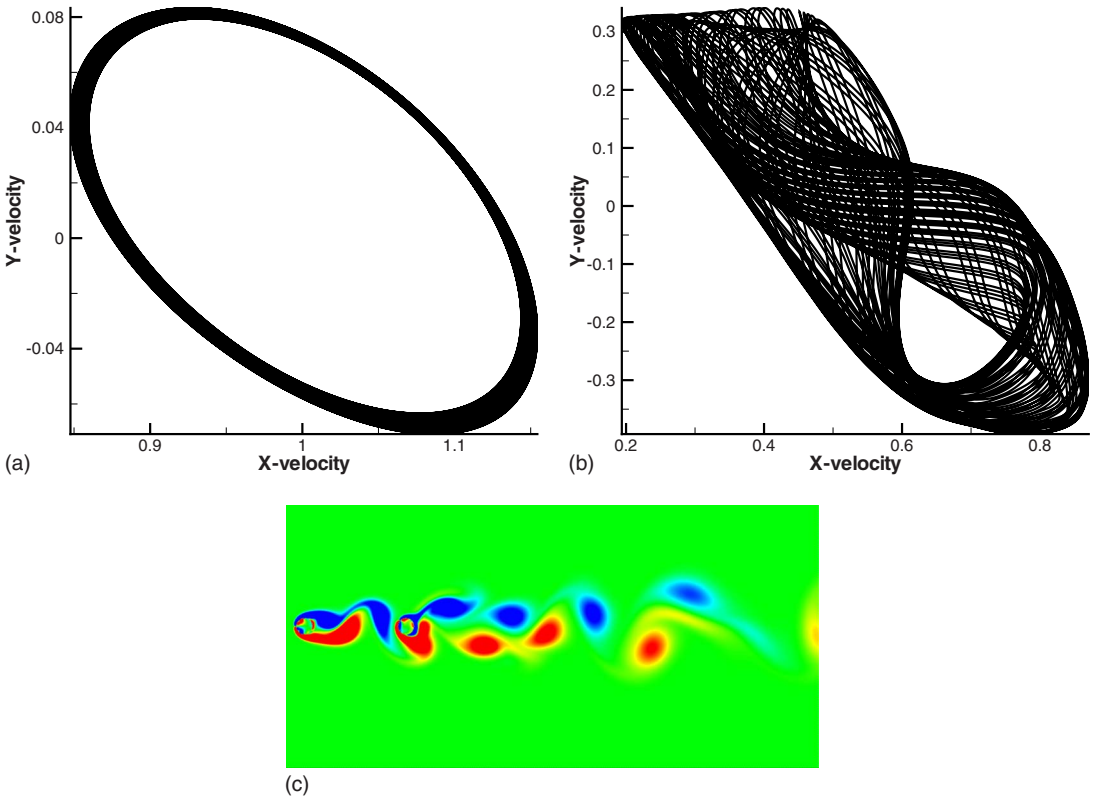

FIG. 14. (Color online) The VF case of $S=6$, $f_c=1.3f_{ns}$, $A=0.15$. (a) Phase portrait plot (upstream cylinder), (b) phase portrait plot (downstream cylinder), (c) vorticity contour plot.

TABLE I. Vortex shedding patterns at $A=0.15$.

	$0.9f_{ns}$	f_{ns}	$1.1f_{ns}$	$1.3f_{ns}$	$1.5f_{ns}$	$1.7f_{ns}$
*S*2	2S	2S	2S	2S	$2S^*$,2S	$2S^*$,2S
*S*4	2S	2S	2S,$2S^*$	2S,$2S^*$	2S,$2S^*$	2S,$2S^*$
*S*6	S+P,$2S^*$	$2S^*$	$2S^*$,S+P,2S	$2S^*$,S+P,2S	$2S^*$,S+P,2S	$2S^*$

wake between the two cylinders does not yet develop clear vortex shedding, and therefore even vorticity contours of the wake behind the upstream in Fig. 10(c) look similar to those in Fig. 8(c).

If we increase the amplitude to 0.35, the system is no longer locked-in at any excitation frequency. In the power spectrum plots for $S=4$ at $0.9f_{ns}$ in Fig. 7(a), a dominant peak at the excitation frequency of $0.9f_{ns}$ still exists in the upstream wake, absent any clearly significant peaks at its harmonics. This type of non-lock-in spectra was also discovered by Karniadakis and Triantafyllou[2] for a single oscillating cylinder case as a flow state between the states occurring in lock-in and non-lock-in cases. When we look at the corresponding velocity phase portraits in Fig. 11(a), they are no longer single orbits but multiple loops instead, although they are not totally chaotic. This shows that this state is not far away from the state in a lock-in case, and the flow with this type of phase portraits is categorized as transitional by Ref. 1. It should be noted that in all the lock-in cases, steep (narrow band), significant peaks appear at the excitation frequency as well as its harmonics. The upstream wake has one more interesting feature: no peaks appear at high frequencies. The absence of peaks at higher frequencies in the velocity spectra of the upstream wake occurs in all the non-lock-in cases for larger spacing with $S=4$ and $S=6$. The reason, as stated earlier, is because the high-frequency peaks in the downstream wake are generated by interactions between the upstream wake and the oscillating downstream cylinder, and such interactions only have weak influences on the upstream wake when the spacing is large. For the downstream wake in this case, as shown in Fig. 7(a), a peak also appears at the natural frequency f_{ns} in addition to the peak that appears at the excitation frequency of $0.9f_{ns}$, and peaks appear at the harmonics of these two frequencies. Therefore, the velocity phase portraits in Fig. 11(b) show a more chaotic, quasiperiodic response state.

We can now compare the flow structures at the two amplitudes at $0.9f_{ns}$, one a lock-in case ($A=0.15$) and the other a transitional case ($A=0.35$). For $A=0.15$ in Fig. 10(c), no clear vortex shedding occurs in the wake of the upstream cylinder, and the vortex street in the wake of the downstream cylinder is a 2S structure. For $A=0.35$ in Fig. 11(c), vortex shedding starts to appear in the upstream wake. The downstream near wake is 2S, and changes to $2S^*$ in the far wake. The 2S structures are typical in lock-in and transitional states, and not so much in quasiperiodic states, as evident in other studies.[1,2]

Increasing excitation frequency to $1.1f_{ns}$ and higher leads to non-lock-in states for all the cases of $S=4$. For $A=0.15$ in Fig. 4, the upstream wake goes through a transitional state at $f_c=1.1,1.3,1.5f_{ns}$ to a quasiperiodic state at $f_c=1.7f_{ns}$, while the downstream wake reaches a quasiperiodic state directly starting at $f_c=1.1f_{ns}$. We use $f_c=1.3f_{ns}$ as an example. The velocity phase portraits in Figs. 12(a) and 12(b) show that the upstream wake and downstream wake are in different response states: the former is transitional and the latter quasiperiodic. The power spectra in Fig. 6(d) show that two major peaks coexist at f_{ns} and $1.3f_{ns}$ in the downstream spectrum (the solid black curve), while one significant but not so narrow-banded peak appears at f_{ns} in the upstream wake spectrum. In addition, the upstream wake spectrum does not acquire high frequency peaks as the downstream spectrum does. The vorticity field still shows a $2S+2S^*$ structure in Fig. 12(c), which is not much different from the lock-in case of $f_c=0.9f_{ns}$, $A=0.15$.

At $A=0.35$ and $f_c=1.3f_{ns}$, both the downstream and upstream wakes are in quasiperiodic states. In Fig. 7(d), peaks at f_{ns} and $f_c(=1.3f_{ns})$ coexist in both the upstream and downstream wakes. In this case, although the upstream phase portrait in Fig. 13(a) shows an orbital behavior that can be viewed as being close to a transitional state, the spectrum is thus used to identify it as a quasiperiodic state. Like other phase portraits in the paper, this behavior of the phase portraits is processed based on the result of a long-time simulation until the solution converges to a state that shows periodic oscillations. In this case, the vorticity field, the $2S+2S^*$ structure in Fig. 13(c), also does not differ much from that of the lock-in cases. The high-frequency peaks shown in the downstream wake are still absent in the upstream wake.

TABLE II. Vortex shedding patterns at $A=0.35$.

	$0.9f_{ns}$	f_{ns}	$1.1f_{ns}$	$1.3f_{ns}$	$1.5f_{ns}$	$1.7f_{ns}$
*S*2	2S	2S	2S	2S	$2S^*$,2S	$2S^*$,S+P,2S
*S*4	2S,$2S^*$	2S	2S,$2S^*$	2S,S+P	2S,$2S^*$,S+P	2S,$2S^*$
*S*6	$2S^*$,2S	S+P,2S	$2S^*$,2S	S+P,2S	$2S^*$,2S	S+P,2S

C. The VF spacing, $S=6$

The essential difference between the VS and VF cases is the distance between the two cylinders, for which the larger spacing leaves more space for vortex shedding to develop, and the vortex street behind the tandem cylinders is from coupled upstream and downstream wakes. As a result, in Figs. 4 and 5, there is no lock-in at this spacing; at all the excitation frequencies and amplitudes, the upstream wake is in a transitional state and the downstream wake in a quasiperiodic state. The high-frequency peaks are absent in the upstream wake in all the cases. We look at the case of $A=0.15$, $f_c=1.3f_{ns}$ as an example. In Figs. 14(a) and 14(b), the phase portraits for the upstream and downstream wakes are in typical transitional and quasiperiodic states, respectively. The velocity spectra in Fig. 6(d) show typical a transitional and a quasiperiodic spectrum each for the upstream and downstream wakes: the upstream wake has a peak at the natural frequency in a relatively broadband manner but no significant peak at the excitation frequency, while the downstream wake has peaks at both natural and excitation frequencies. In all the VF cases, the vorticity field of the upstream wake is mostly 2S, while the downstream wake has a combination of 2S, $2S^*$, and S+P. As shown in Fig. 14(c), the downstream wake reveals both $2S^*$ and S+P structures. It should be noted that based on our results, the S+P structures only occur in the quasiperiodic cases; however, not all the quasiperiodic cases show the S+P structures, and some of them are only 2S and $2S^*$. On the other hand, all the lock-in cases are only 2S, and the transitional cases are combination of 2S and $2S^*$. Here we present a summary of the vortex shedding patterns using Tables I and II below for the two amplitudes. Based on these tables, we find that the vorticity field can be used to distinguish between lock-in and non-lock-in cases, but cannot be used to distinguish transitional from quasiperiodic cases.

V. CONCLUSIONS

For flow over a stationary tandem cylinder system, three flow regimes occur according to the wake development stage behind the upstream cylinder: VS, critical, and VF. Each depends on the spacing distance between the two cylinders. When the downstream cylinder oscillates transversely at a frequency in the vicinity of the Strouhal number of the corresponding stationary tandem cylinder system with a small amplitude as the cases in this study ($A<0.5D$), these flow regimes do not change; however, the state of the nonlinear response varies in different flow regimes. We categorize these response states into three classes: lock-in, transitional, and quasiperiodic, each reflecting the order of increasing levels of chaotic response. For a flow Reynolds number of 100, we investigated the excitation frequencies in the range from $0.9f_{ns}$ to $1.3f_{ns}$ and amplitudes of $0.15D$ and $0.35D$. The velocity histories were recorded at the near-wake regions behind each of the cylinders. We analyzed response state diagrams, velocity spectra, velocity phase portraits, and vorticity fields for these cases.

For different flow regimes at different spacing distances between the two cylinders, we find that the VS regime has a wider frequency or amplitude range of lock-in than the critical and VF regimes, and the response states are not sensitive to the excitation amplitude in this regime. The upstream and downstream wakes are in the same response state for all the cases because of the close spacing between the two cylinders. The critical regime can include lock-in, transitional, and quasiperiodic states at different excitation frequencies at low amplitudes. For higher amplitudes, no lock-in exists in the critical regime. For the VF regime at all the frequencies and amplitudes that we have studied, the upstream wake remains transitional and the downstream wake quasiperiodic, and there is no lock-in state. There is no transitional state at the downstream wake in both critical and VF regimes.

The near-wake velocity spectral behaviors correspond to the nonlinear response states. For the lock-in state, narrow-banded peaks appear at the excitation frequency and its harmonics. These narrow-banded peaks are related to a clearly 2S-type vortex shedding pattern in the wake behind a lock-in tandem cylinder system. For the transitional state, a peak appears at either the excitation frequency or the natural frequency or at a frequency in between the two. This peak is not so narrow banded as in the lock-in state, and narrow-banded peaks do not appear at the harmonics either. The vorticity structure in the wake starts to show $2S^*$-type vortices, along with some 2S vortices. For the quasiperiodic state, peaks appear at both the excitation and natural frequencies. The vorticity structure in the wake for the quasiperiodic state can have a combination of 2S, $2S^*$, as well as S+P-type vortices. Except for the two lock-in cases at the critical regime, the upstream wake spectra in all the cases at critical and VF spacing do not have high frequency harmonic peaks, as opposed to the corresponding downstream wake spectra.

Among phase portraits, velocity spectra, and vorticity structures, the combination of the former two is able to accurately determine the state of the tandem cylinder system within the three nonlinear response states studied here. Vorticity structures, on the other hand, cannot be used to accurately distinguish the response state, although there are some wake vortex structures pertaining to certain nonlinear states.

In summary, for a transversely oscillating cylinder in a wake of a stationary cylinder, the general trend in these nonlinear responses is that the larger the spacing distance, the higher the excitation frequency and amplitude, the more chaotic the flow becomes. The critical regime is most sensitive to the change in excitation frequency and amplitude. The VF regime does not seem to allow any lock-in regardless of the frequency and amplitude. As the above statements are made based on flow at the Reynolds number of 100, they are possibly applicable for flow in a range of Reynolds numbers near 100.

[1] G. V. Papaioannou, D. K. P. Yue, M. S. Triantafyllou, and G. E. Karniadakis, "Evidence of holes in the Arnold tongues of flow past two oscillating cylinders," Phys. Rev. Lett. **96**, 014501 (2006).
[2] G. E. Karniadakis and G. S. Triantafyllou, "Frequency selection and asymptotic states in laminar wakes," J. Fluid Mech. **199**, 441 (1989).
[3] Z. C. Zheng and N. Zhang, "Frequency effects on lift and drag for flow past an oscillating cylinder," J. Fluids Struct. **24**, 382 (2008).
[4] R. E. D. Bishop and A. Y. Hassan, "The lift and drag forces on a circular cylinder oscillating in a flowing fluid," Proc. R. Soc. London, Ser. A **277**, 51 (1964).

[5]C. H. K. Williamson and A. Roshko, "Vortex formation in the wake of an oscillating cylinder," J. Fluids Struct. **2**, 355 (1988).
[6]S. Krishnamoorthy, S. J. Price, and M. P. Paidoussis, "Cross-flow past an oscillating circular cylinder: Synchronization phenomena in the near wake," J. Fluids Struct. **15**, 955 (2001).
[7]M. M. Zdravkovich, *Flow Around Circular Cylinders* (Oxford University Press, New York, 1997).
[8]P. Anagnostopoulos, "Numerical study of the flow past a cylinder excited transversely to the incident stream. Part 1: Lock-on zone, hydrodynamic forces and wake geometry," J. Fluids Struct. **14**, 819 (2000).
[9]E. Guilmineau and P. Queutey, "A numerical simulation of vortex shedding from an oscillating circular cylinder," J. Fluids Struct. **16**, 773 (2002).
[10]M. M. Zdravkovich, "Flow-induced oscillations of two interfering circular cylinders," J. Sound Vib. **101**, 511 (1985).
[11]Y. Tanida, A. Okajima, and Y. Watanabe, "Stability of a circular cylinder oscillating in uniform flow or in a wake," J. Fluid Mech. **61**, 769 (1973).
[12]J. Li, A. Chambarel, M. Donneaud, and R. Martin, "Numerical study of laminar flow past one and two circular cylinders," Comput. Fluids **19**, 155 (1991).
[13]B. Sharman, F. S. Lien, L. Davidson, and C. Norberg, "Numerical predictions of low Reynolds number flows over two tandem circular cylinders," Int. J. Numer. Methods Fluids **47**, 423 (2005).
[14]J. Deng, A.-L. Ren, J.-F. Zou, and X.-M. Shao, "Three-dimensional flow around two-circular cylinders in tandem arrangement," Fluid Dyn. Res. **38**, 386 (2006).
[15]G. V. Papaioannou, D. K. P. Yue, M. S. Triantafyllou, and G. E. Karniadakis, "Three-dimensionality effects in flow around two tandem cylinders," J. Fluid Mech. **558**, 387 (2006).
[16]J. Li, J. Sun, and B. Roux, "Numerical study of an oscillating cylinder in uniform flow and in the wake of an upstream cylinder," J. Fluid Mech. **237**, 457 (1992).
[17]N. Mahir and D. Rockwell, "Vortex formation from a forced system of two cylinders. 1. Tandem arrangement," J. Fluids Struct. **10**, 473 (1996).
[18]A. Ongoren and D. Rockwell, "Flow structure from an oscillating cylinder. Part 1. Mechanisms of phase shift and recovery in the near wake," J. Fluid Mech. **191**, 197 (1988).
[19]R. Govardhan and C. H. K. Williamson, "Modes of vortex formation and frequency response of a freely vibrating cylinder," J. Fluid Mech. **420**, 85 (2000).
[20]R. Govardhan and C. H. K. Williamson, "Mean and fluctuating velocity fields in the wake of a freely-vibrating cylinder," J. Fluids Struct. **15**, 489 (2001).
[21]G. V. Papaioannou, D. K. P. Yue, M. S. Triantafyllou, and G. E. Karniadakis, "On the effect of spacing on the vortex-induced vibrations of two tandem cylinders," J. Fluids Struct. **24**, 833 (2008).
[22]T. L. Morse and C. H. K. Williamson, "Employing controlled vibrations to predict fluid forces on a cylinder undergoing vortex-induced vibration," J. Fluids Struct. **22**, 877 (2006).
[23]T. L. Morse and C. H. K. Williamson, "Fluid forcing, wake modes and transitions for a cylinder undergoing controlled oscillations," J. Fluids Struct. **25**, 697 (2009).
[24]N. Zhang and Z. C. Zheng, "An improved direct-forcing immersed-boundary method for finite difference applications," J. Comput. Phys. **221**, 250 (2007).
[25]C. H. K. Williamson, "Vortex dynamics in the cylinder wake," Annu. Rev. Fluid Mech. **28**, 477 (1996).
[26]T. Leweke, M. Provansal, G. D. Miller, and C. H. K. Williamson, "Formation in cylinder wakes at low Reynolds numbers," Phys. Rev. Lett. **78**, 1259 (1997).